ChemPubSoc Europe

DOI: 10.1002/chem.201705655

CHEMISTRY A European Journal Full Paper

Hydrogen Evolution

Bioinspired Electro-Organocatalytic Material Efficient for Hydrogen Production

Octavio González-del Moral,[a, b] Arnau Call,[c] Federico Franco,[d] Alicia Moya,[a] Jose Antonio Nieto-Rodríguez,[a] María Frias,[e] Jose L. G. Fierro,[g] Miquel Costas,[c] Julio Lloret-Fillol,[d, h] José Alemán,[e, f] and Rubén Mas-Ballesté*[a, f]

Abstract: Commercial carbon fibers can be used as electrodes with high conductive surfaces in reduced devices. Oxidative treatment of such electrodes results in a chemically robust material with high catalytic activity for electrochemical proton reduction, enabling the measurement of quantitative faradaic yields (>95%) and high current densities. Combination of experiments and DFT calculations reveals that the presence of carboxylic groups triggers such electrocatalytic activity in a bioinspired manner. Analogously to the known Hantzsch esters, the oxidized carbon fiber material is able to transfer hydrides, which can react with protons, generating H_2, or with organic substrates resulting in their hydrogenation. A plausible mechanism is proposed based on DFT calculations on model systems.

Introduction

Nicotinamide adenine dinucleotide phosphate, which is abbreviated as $NADP^+$ (oxidized form) and NADPH (reduced form), is a coenzyme that is involved in a large number of biological processes (Figure 1 A and B).[1,2] NADPH provides one of the best reducing biological agents for a large variety of bioreduction reactions (Figure 1, left), which nature uses in a catalytic manner. Interestingly, inspired by NADPH, the asymmetric transfer hydrogenation from Hantzsch esters (**C**) has appeared as a green alternative for the reduction of C=C, C=N, and C=O bonds (Figure 1, middle).[3–10] In this case, the reductive form (**C**) is easily oxidized to the pyridine derivative (**C'**) through a hydride-transfer process. Some important drawbacks of these synthetic reagents, such as their difficult recovery due to its challenging purification, the need for superstoichiometric amounts (>2 equiv) and the high cost, all complicate the implementation of these reagents in industry. Consequently, it would be highly desirable to find a new technology that can

[a] Dr. O. G.-d. Moral, Dr. A. Moya, J. A. Nieto-Rodríguez, Dr. R. Mas-Ballesté
Department of Inorganic Chemistry (module 07)
Facultad de Ciencias, Universidad Autónoma de Madrid
28049 Madrid (Spain)
E-mail: ruben.mas@uam.es

[b] Dr. O. G.-d. Moral
Department of Chemistry (module 13), Facultad de Ciencias
Universidad Autónoma de Madrid, 28049 Madrid (Spain)

[c] Dr. A. Call, Dr. M. Costas
Departament de Química and Institute of Computational Chemistry and Catalysis (IQCC), Universitat de Girona
Campus Montilivi, 17071 Girona, Catalonia (Spain)

[d] Dr. F. Franco, Dr. J. Lloret-Fillol
Institute of Chemical Research of Catalonia (ICIQ)
The Barcelona Institute of Science and Technology
43007 Tarragona, Catalonia (Spain)

[e] M. Frias, Dr. J. Alemán
Department of Organic Chemistry (module 01)
Universidad Autónoma de Madrid, 28049 Madrid (Spain)

[f] Dr. J. Alemán, Dr. R. Mas-Ballesté
Institute for Advanced Research in Chemical Sciences (IAdChem)
Universidad Autónoma de Madrid, 28049 Madrid (Spain)

[g] Dr. J. L. G. Fierro
Instituto de CatálisisyPetroleoquímica, CSIC
Marie Curie 2, Cantoblanco, 28049 Madrid (Spain)

[h] Dr. J. Lloret-Fillol
Catalan Institution for Research and Advanced Studies (ICREA)
Passeig Lluïs Companys 23, 08010 Barcelona (Spain)

Supporting information and the ORCID number for the author of this article can be found under https://doi.org/10.1002/chem.201705655.

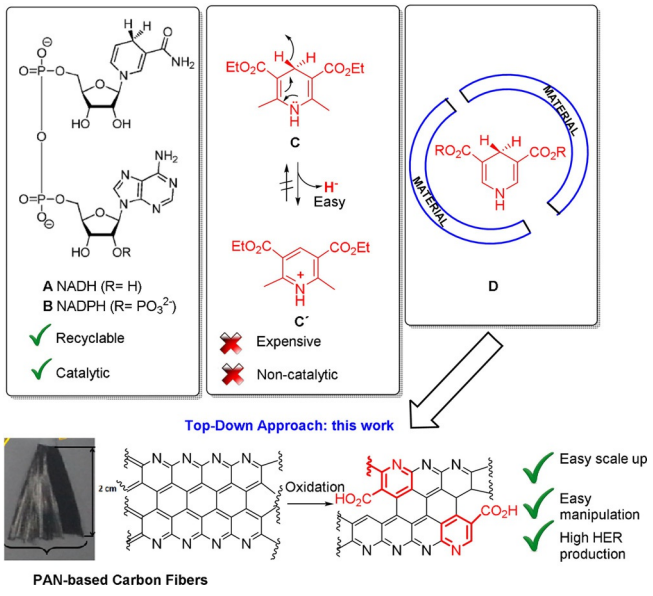

Figure 1. Inspiration and initial goals of this work.

be used to incorporate this type of species into a material (Figure 1 D), thereby overcoming the problems associated with Hantzsch ester derivatives.

One of the processes that could be facilitated by a material incorporating structures acting as hydride-transfer mediators is the hydrogen-evolution reaction (HER). In this context, the hydrogen evolution reaction is a main target in modern chemistry because it can represent a change in the energy production paradigm. In fact, hydrogen is envisioned to be an abundant, renewable and zero-emission fuel that could replace fossil fuels.[11] Water electrolysis is one of the simplest ways to produce hydrogen of high purity and thus it has attracted considerable attention.[12] This process requires new electrocatalysts to improve the production rates and decrease overpotentials. HER electrocatalysts can be homogeneous or heterogeneous.[13,14] For homogeneous molecular catalysts, application requires their stable grafting onto electrode materials. Such a problem could be solved by using heterogeneous systems, which are generally more stable and easier to implement into devices. Pt-group metals are excellent heterogeneous HER catalysts, but their wide use is limited by their terrestrial scarcity and high price.[15,16] Thus, investigations in precious-metal-free catalysis[17] or even metal-free catalysis[18] are being developed with the aim to obtain acid-stable (since conditions to generate H_2 usually require acidic conditions) and highly active catalysts for HER based on inexpensive earth-abundant materials (such as carbon-based materials).

Carbon-based materials can be produced on a large scale with lower manufacturing cost compared with metal-based materials.[19–21] In addition, carbonaceous materials often offer synergy between the material and attached active centers due to the electrical conductivity and the electron acceptor/donor properties of graphitic structure such as graphene or carbon nanotubes.[22] Therefore, carbon-based materials are very attractive alternatives to conventional heterogeneous electrocatalysts used for hydrogen evolution and other electrochemical reactions.[23,24] They are attractive not only from the economic point of view, but also from a scientific side. In fact, whereas HER pathways catalyzed by metals have been widely studied,[25,26] much less is known about the catalytic mechanism for H_2 formation in metal-free materials. Following these ideas, in recent work, carbon nanotubes and other modified graphene/graphitic materials have been explored as electrocatalysts in HER.[22,27–32] Some of these contributions described deposition of carbon nanotubes, or functionalized graphene, on small surface area glassy carbon electrodes.[33] Good overpotential and current intensity values have been reported. However, in some cases, the results were limited by common problems, such as adhesion of deposited phases into the electrode surface or the small area of such electrodes, which compromised absolute yields of produced hydrogen. In general, the price, the manipulation of these carbon nanostructures, the deposition onto a substrate material (e.g., glass), and the small scale of these nanostructures limit the production of hydrogen. Therefore, it would be very convenient to find another appropriate carbon-based structure for large-scale electrocatalytic HER.

Inspired by these findings, we propose in this report an inexpensive and easy-to-handle alternative that consists of the use of commercially available carbon fibers from pyrolysis of polyacrylonitrile (PAN).[34] This material has a well-established structure,[35] which includes pyridyl fragments (Figure 1, right and bottom), and can be oxidized to form acid derivatives.[36,37] If such carboxylic groups are in the *meta*-position in the pyridine ring the resulting structure is a nicotinic fragment. In that case, it can act like $NADP^+$ (oxidized form) and NADPH (reduced form) in electrochemical systems; that is, as hydride-transfer agents in HER processes. Here we report that this material can be easily handled and oxidized to be used for HER in large quantities. Moreover, a novel plausible mechanism (through hydride-transfer) has been proposed based on a combination of experimental observations and DFT calculations.

Results and Discussion

Preparation and characterization of the catalytic material

In this work, carbon fibers are considered as a good material for the design of electrocatalysts because they allow the fabrication of high surface area and covalently stable functionalized electrodes. This approach avoids drawbacks such as the inconvenience of working with reduced amounts of material at a nanometric scale.[18,38–40] According to the manufacturer, the carbon fiber material consists of bundles of 3000 fibers[34] with each fiber having an average diameter of 8 μm. We designed electrodes in a brush disposition (details of the electrode design are provided in Figure S1 of the Supporting Information). In a typical configuration, we used a brush composed of 42 000 fibers with an exposed length of 2 cm. This design implies that, if aggregation does not take place at all and every fiber behaves independently from each other, the theoretical maximum available surface area of the carbon fiber is approximately 2100 cm^2 (for evaluation of catalytic active surface area see below). This is a remarkable feature that is important for reduced device size. Moreover, the high conductivity of such carbon fibers effectively enables their use as efficient electrodes. A main advantage of this new design is the extremely low price of the carbon material. However, not only the price, but also the special chemical features of this material make carbon fibers very attractive.[39,41]

Oxidative procedures are expected to affect only the surface of the material. Accordingly, although superficial properties are changed (interaction with polymeric matrices or, as shown below, electrocatalytic behavior), bulk features remain unaltered (mechanical and electrical properties). Therefore, characterization of the chemical modification resulting from oxidative procedure should be performed using a technique specifically sensitive to surface chemical features. Thus, comparative spectroscopic study of pristine and oxidized fibers was performed by means of XPS (Figure 2). Comparison of XPS spectra in the C 1s region between pristine carbon fibers and highly oriented pyrolytic graphite (Figure 2 HOPG, top) indicated that carbon fibers are a less structured material, as can be deduced from the increased broadness of C–C signal (284–285 eV) and the

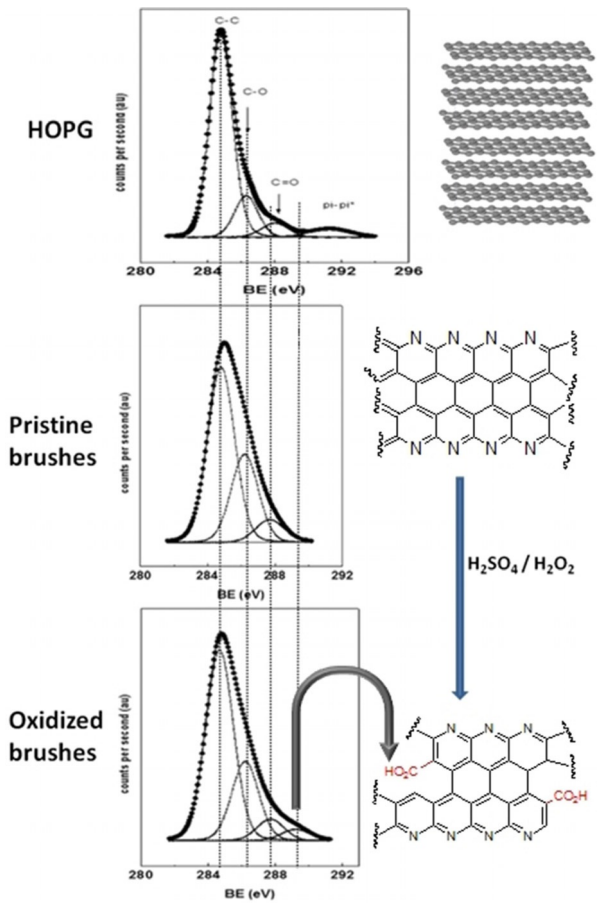

Figure 2. C 1s core-level spectra corresponding to pristine HOPG, pristine carbon fibers, and oxidized carbon fibers.

lack of signal in the region characteristic of stacked materials with large π–π interactions (291–293 eV). An increase of the C–O (286.2 eV) and C=O (287.7 eV) signals are also observed in the carbon fiber, especially in the oxidized one. Although these signals can, to a certain extent, be due to adhesion of adventitious organic molecules, they are mostly indicative of the degree of chemical functionalization. Such structural imperfections and the polarization of the material by the pyridine moieties facilitate a chemical functionalization by oxidizing over H_2SO_4/H_2O_2 (1:1). Such reactivity has previously been reported for modification of carbon fibers to increase their interaction with polymeric matrices.[42–44]

Although harsh, such conditions are known to be innocuous to graphite, which needs harsher conditions to be transformed into graphene oxide.[45] After the oxidation process, the electric conductivity was not lost, as measured with a macroscopic multimeter. This is a good indication that the bulk properties of fibers are not altered. Accordingly, the morphology of the carbon fiber has not been considerably modified during the oxidation treatment (Figure S2). However, an alteration of the chemical composition of carbon fibers is determined by XPS. This analysis revealed the presence of highly oxidized carbon atoms (O-C=O) at 289.1 eV, which were assigned to carboxylic groups resulting from the oxidative process. On average, 5% of the carbon atoms in the surface correspond to carboxylic groups. Therefore, considering that the maximum number of catalytic centers is close to the number of carboxylic groups (see below), the approximate active area can be, at most, 5% of the available electrode surface. To discard the possible role of adventitious metal centers in the catalytic activity (see below), we recorded XPS survey spectra, which did not show the presence of metal atoms (Figure S10). In addition, the presence of nitrogen atoms from pristine material was also identified in oxidized fibers by means of the XPS signal at a binding energy of 401.9 eV, which can be assigned to pyridinic nitrogen atoms. Furthermore, total reflection X-ray fluorescence (TXRF) analysis was performed to analyze the oxidized fiber (Figure S11). Only a small content of Si and Cu (below the ppm level) were found, which is not significant to account for catalytic activity.

Thus, overall, C 1s and N 1s XPS signals, together with TXRF analytical data, SEM microscopy images, and electric characterization are all consistent with our previous assumption. Therefore, experimental data suggest that although oxidation does not result in significant changes in bulk properties and morphology, it produces limited changes in the chemical features of the surfaces consisting of generation of carboxylic groups, which can result in transformation of pyridinic fragments into nicotinic structures.

Electrocatalytic behavior

The effect of the oxidative process on the electrochemical behavior of carbon fiber brushes was analyzed towards proton reduction in CH_3CN, using dilute solutions of trifluoroacetic acid (CF_3COOH; TFA) as proton donor and 0.1 M $N(Bu)_4PF_6$ as inert electrolyte. This electrolyte system allowed the catalytic performance of oxidized brushes in low proton content solutions to be evaluated, avoiding saturation of signal in a wide range of electrochemical potentials. In addition, experiments using controlled variable amounts of proton source have also enabled us to determine at what point all catalytic sites arrive

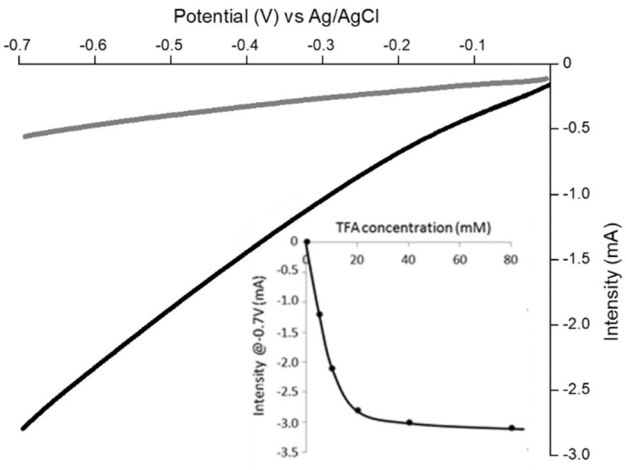

Figure 3. Typical response of pristine (gray line) and oxidized (black line) electrodes in CH_3CN (0.1 M $N(Bu)4PF_6$) with TFA 20 mM. Inset: electrochemical response of oxidized electrode with variable amounts of TFA (scan rate: 10 mV s^{-1}).

at the saturation point. Figure 3 shows a typical linear-sweep voltammetry plot measured for a 20 mM solution of TFA using both pristine (gray line) and oxidized electrodes (black line) between 0.0 and −0.7 V vs. Ag/AgCl at a scan rate of 10 mV s^{-1}. The observed cathodic current was significantly increased because of the oxidative functionalization process on the carbon fiber electrodes (black line). The measured current intensity depends on the TFA concentration, with a higher proportionality factor at lower acid amounts, indicating the saturation of all catalytic sites at higher TFA content (inset Figure 3). Overall, oxidized carbon fibers show a remarkable catalytic activity towards proton reduction, whereas pristine electrodes do not show such activity.

Formation of H_2 was tested using an airtight cell and quantitatively detected by gas chromatography (GC) (see Figure 4). Controlled-potential electrolysis was performed at $E=-0.9$ V vs. Ag/AgCl in a 0.1 M $TBAPF_6/CH_3CN$ solution by using the oxidized carbon fiber as the working electrode in the presence of 20 mM TFA as the proton source. The electrocatalytic reaction provided an average faradaic efficiency $>95\%$ for H_2 during 1 h of experiment. After that time, hydrogen production stops. However, a freshly added aliquot of TFA (identical to the starting one, corresponding to ca. 20 mM) restored the electrocatalytic H_2 production, providing analogous results in terms of both faradaic efficiency and mmol of H_2 produced for another hour (Figure 4). This clearly demonstrates the capability of the oxidized carbon fiber in the catalysis of H_2 evolution reaction under acidic conditions, whereas similar experiments using a pristine electrode did not show any evidence of H_2 formation.

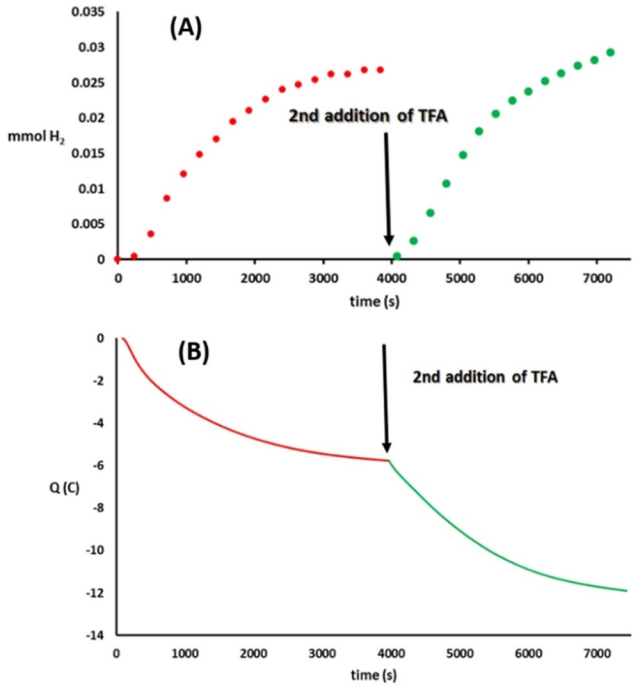

Figure 4. a) Electrocatalytic H_2 evolution over time at $E=-0.9$ V vs. Ag/AgCl in a 0.1 M $TBAPF_6/CH_3CN$ solution of carbon fiber in the presence of added 20 mM TFA. The same volume of fresh TFA was injected after ca. 1 h of experiment. b) Charge passed in the course of the electrocatalytic H^+ reduction at $E=-0.9$ V vs. Ag/AgCl in a 0.1 M $TBAPF_6/CH_3CN$ solution of carbon fiber upon addition of two distinct aliquots of TFA (20 mM).

As explained above, considering the design applied to brush electrodes, the maximum area available considering all the microfibers independent from each other is 2100 cm^2. However, aggregation of fibers would reduce the available surface. The effect of aggregation was evaluated by comparing the performance of an oxidized electrode composed by few fibers with a regular one. In particular, the experiment was carried out with 54 fibers and 47 fibers (see the Supporting Information, Figure S3). Assuming that with these electrodes the effect of aggregation is negligible and considering that the electrochemical signal is directly proportional to the available electrode area, the available area in the complete brush was determined to be approximately 40 cm^2 (see details in the Supporting Information). Considering that only 5% of the available area is, in fact, active (see XPS data on carboxylic content), the overall active area would be approximately 2 cm^2, which is the electrode area used to calculate current densities in the following experiment of this work.

Although data obtained in CH_3CN was very insightful, it is neither the ideal working medium nor the standard conditions used in comparable studies reported in the literature. Therefore, as a benchmarking experiment and to compare our system (pristine and oxidized electrodes) with previously reported data, we performed the proton reduction experiments in 0.5 M H_2SO_4 aqueous solution. Figure 5 shows the current

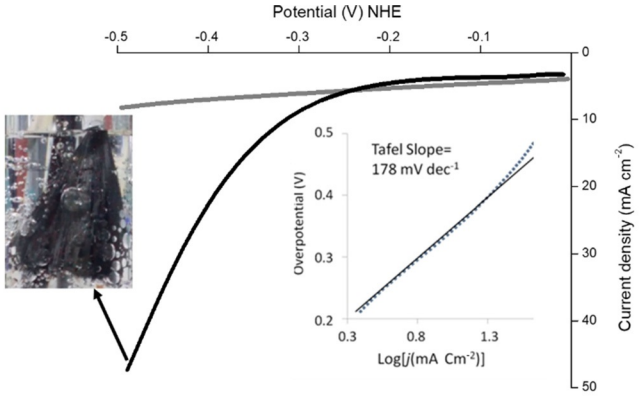

Figure 5. Typical response of pristine (gray line) and oxidized (black line) electrodes in aqueous 0.5 M solution of H_2SO_4 (scan rate: 10 mV s^{-1}). As insets are shown the corresponding Tafel plot and a photograph of the massive hydrogen production observed at 0.5 V vs. NHE.

densities (considering active area = 2 cm^2) measured for linear sweep at potentials between −0.224 and −0.724 V vs. Ag/AgCl (corresponding to the range between 0.0 and −0.5 V vs. NHE) at a scan rate of 10 mV s^{-1}. In this experiment, the major activity of oxidized electrode compared with pristine electrode is clear. An onset overpotential of 250 mV with a Tafel slope of 178 mV dec^{-1} is observed. Although the value of the slope in the Tafel plot is indicative of a process quite hampered kinetically, a current density of 20 mA cm^{-2} was achieved at an overpotential lower than 400 mV. Such relative intensity value is comparable to other electrocatalytic HER using modified carbon based electrodes (see Figure S4 in the Supporting Information).[24] However, considering the large active area found, our absolute currents overcome those reported on a lab-scale

device. In fact, the hydrogen production at overpotential of 0.5 V was massive, as can be observed in the inset picture of Figure 5.

The durability of these electrodes was tested by applying 1000 cycles from 0.0 to −1.0 V vs. Ag/AgCl at 100 mV s^{-1} on a 100 mM solution of TFA in CH_3CN (0.1 M of NBu_4PF_6). After such test, the activity of electrodes remained unaltered (see the Supporting Information, Figure S5), confirming the attractive potential of the oxidized carbon fiber brush electrode for large-scale HER.

Experimental mechanistic evidence

All observations point out that the oxidation process is critical for the electrocatalytic HER. In particular, according to XPS data, it seems that the presence of carboxylic groups is associated with the catalytic activity of the material. To provide further evidence for this concept, we demonstrated that the effect of oxidation in catalytic activity could be reversed when oxidized electrodes were reduced by treating them with $LiAlH_4$ (see Figure 6 and more details in Scheme S1 and Figure S6 in the Supporting Information).

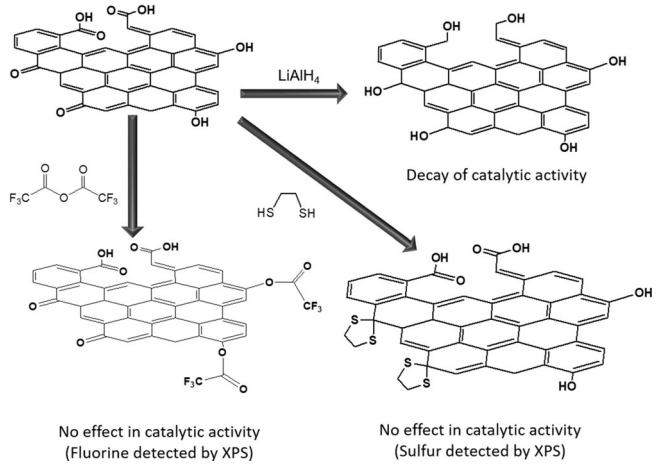

Figure 6. Derivatization reactions performed in the experimental mechanistic study.

To discard the possibility that other functional groups act as catalytic centers, we performed selective derivatizations that should affect specifically hydroxyl or carbonyl (aldehydes or ketones) moieties (Figure 6). Due to the difficulty in following the possible reactions considering the C 1s XPS, we introduced functionalities with heteroatoms, and considered the presence and level of such heteroatoms as evidence for the effective transformation of the material (see Table S1–S5 for more details). In particular, reaction with trifluoroacetic anhydride is expected to quantitatively react with hydroxyl groups as has been widely reported.[18,46] Effectively, the relative atomic abundance found for C, O, and F were 83.4, 11.0, and 5.6%, respectively. Therefore, considering the stoichiometry of the reactions from hydroxyl groups to trifluoroacetate esters, approximately 33% of the oxygen atoms present in the sample reacted in this functionalization process (Figure 6, right-bottom). The activity of the oxidized electrode before and after reaction with trifluoroacetic anhydride was evaluated by linear-sweep voltammetry, showing that such treatment did not alter the activity of oxidized electrode (Figure S7). Therefore, the null effect of the trifluoroacetylation process suggested that hydroxyl groups were not responsible for the catalytic activity of oxidized electrodes.

A similar strategy was followed to determine the possible role of carbonyl groups. Reaction with dithioethane results in the transformation of ketones or aldehydes into dithioacetals (left-bottom, Figure 6).[47] The amount of S atoms found after this reaction corresponds to the functionalization of only 5% of the O atoms detected. Therefore, the amount of carbonyl groups in oxidized electrodes is low compared with hydroxyl fragments (33%). The remaining 60% of oxygen content corresponds to carboxylic functionalities, deduced from the fact that 5% of the carbon atoms on the surface are assigned to -COOH. As expected, reaction with dithioethane had no effect on the catalytic activity of this material (Figure S8).

The overall results seem to indicate that oxidation somehow activated the material as electrocatalysts in HER, but the active sites were neither hydroxyl nor carbonyl groups. Carboxylic groups have previously been proposed as the catalytic centers for hydrogen evolving reaction[23] in oxidized carbon nanotubes. Nevertheless, to date, the role of carboxylic groups has not been elucidated. To test the direct involvement of carboxylic groups in electrocatalytic activity, we analyzed the reactivity of oxidized carbon fiber electrodes containing carboxylic groups that have been esterified by reaction with trimethylsilyldiazomethane or CH_3I. Both reactions should result in conversion of the carboxylic groups into their methyl esters (see the Supporting Information for details).[17,48] In any case, no significant decrease in HER catalytic activity was observed (Figure S9). Consequently, although formation of carboxylic groups in the oxidation process is crucial to promote catalytic activity, such activity remains identical regardless of the fact that the carboxylic groups (-COOH) were converted into esters (-COOR), which could indicate that carboxylic groups are necessary but not directly involved in the catalytic process.

Mechanism proposal and DFT calculations

To find a qualitative hint on the mechanism of the HER process, DFT calculations were carried out at the M06-2X/6–311G** level.[22,49–52] A plausible scenario is shown in Scheme 1. As an approximation, we modeled the oxidized carbon fiber as shown in Scheme 1 for species (I). Graphitic surface was modeled by using a fragment composed of four fused aromatic rings (one pyridine and three benzenes) as a compromise between performance and computational cost.[53,54] We introduced a carboxylic group at the *meta*-position of the pyridinic nitrogen to investigate the effect of oxidation, generating a structure similar to the hydride transfer centers found in nature (such as NADPH).

The overall process (see Figure 7) should start with the injection of electrons into the graphitic system. It is known that the

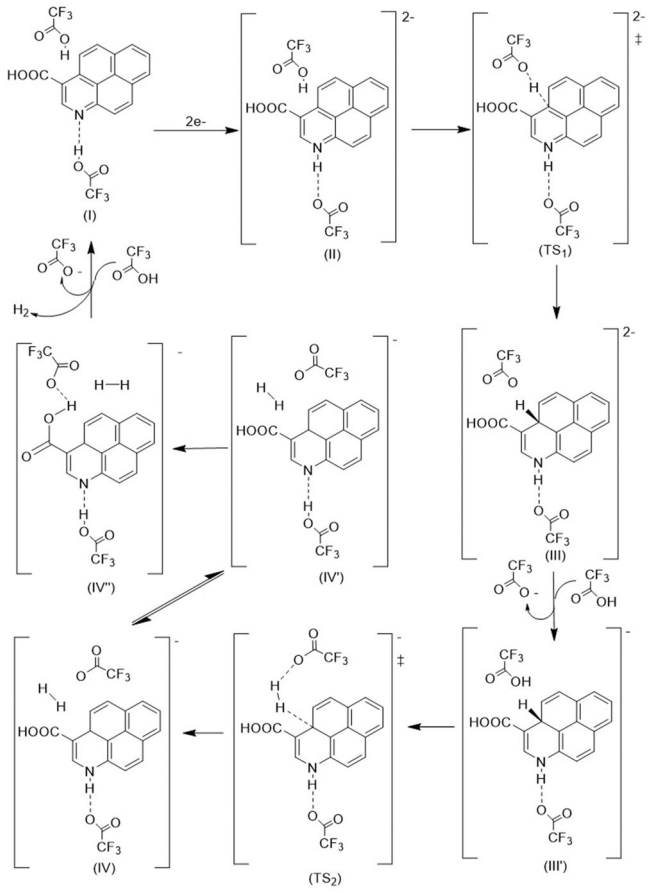

Scheme 1. Mechanistic proposal calculated for hydrogen evolution.

value for the work function of HOPG is about 4.8 eV,[55] which is expected to be close to the value of the carbon fiber material. Stabilization of injected electrons through the graphitic π-electron density is the key factor that allows carbon-based oxidized materials to act efficiently as an electric conductor and as an electrocatalyst. Otherwise, in simple carboxylic molecular systems the first reduction step would be energetically prohibitive. However, considering the reduced size of the structure used in our calculations to simulate the graphenic region, the stabilization energy after injection of two electrons is most likely underestimated. Indeed, injection of two electrons results in a stabilization of 3.13 eV.

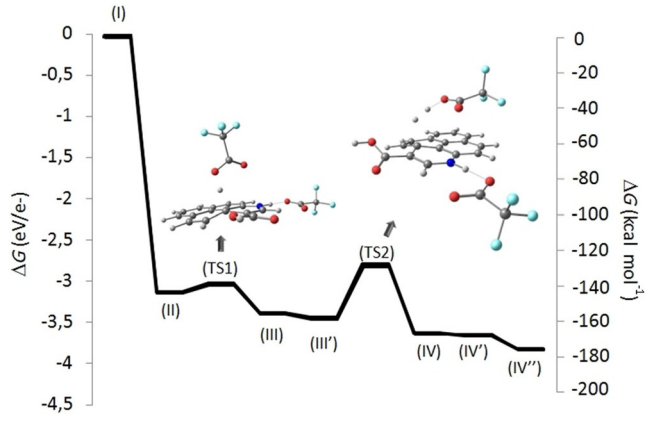

Figure 7. Energetic profile corresponding to the mechanism shown in Scheme 1. Structures of **TS1** and **TS2** are shown.

After injection of two electrons in our molecular model, the negative charge increases the basicity of the pyridinic nitrogen atom. Therefore, calculations suggest that, after two electron injections, the encounter of a TFA molecule with **I** results in a barrierless protonation process. Consequently, the route from **I** to **II** could be described as a proton-coupled electron transfer. In addition, injection of two electrons also enhances the basicity of the carbon *para* to the pyridinic nitrogen in species **II**. Indeed, protonation of **II** proceeds with an activation energy of 4.5 kcal mol^{-1} (**TS1**) and results with an extra stabilization of the system by approximately 12 kcal mol^{-1} in compound **III**.

According to the calculations carried out in our system, intermediate **III** should exchange a trifluoroacetate molecule by trifluoroacetic to generate **III′**. Such exchange is slightly exergonic by around 3 kcal mol^{-1}. Species **III′** evolves towards hydride scission assisted by an acid molecule, resulting in the formation of a hydrogen molecule and trifluoroacetate fragment in species **IV**. Such species is almost isoenergetic with **IV′**, only 0.4 kcal more stable than **IV** and therefore, in this system the pyridine protonation is in equilibrium with the protonation of a trifluoroacetate. Furthermore, in the most stable final structure **IV′′** the trifluoroacetate fragment is stabilized by hydrogen bonding with the carboxylic group of the nicotinic moiety. Formation of **IV**/**IV′** proceeds through a significant kinetic barrier (approximately 30 kcal mol^{-1}), which is similar to values found for reactions mediated by the biomimetic Hantzsch ester.[56] Given that this is the only step with a significant kinetic barrier, it is clearly the rate-determining step of the overall process. The finding of a relatively high barrier is in agreement with the high Tafel slope experimentally measured, which suggested a kinetically hampered process. In addition, oversimplification of the molecular system considered to simulate the material can contribute to barrier overestimation. The studied mechanism considers the assistance of a TFA molecule in the hydride scission, decreasing the value of the energetic barrier by 17 kcal mol^{-1} with respect to the unassisted hydride formation (see the Supporting Information). However, more complex possibilities in which several TFA and/or water molecules could assist hydride formation and stabilize the transition state have not been computed; nevertheless, they are plausible scenarios in the experimental system. In conclusion, theoretical and experimental results are consistent with a mechanism in which the key step consists of the TFA-assisted formation of a hydride from species **III** that is concertedly protonated to generate hydrogen.

Furthermore, the notion that oxidation is needed to favor the catalytic activity is reinforced by the calculations performed in the system in which the carboxylic group is substituted by a hydrogen atom (mechanism b in the Supporting Information). In this case, intermediate species show higher energies than their oxidized counterparts, which is due to the extra conjugation added to the system by the carboxylic groups. In addition, the possible role of carboxylic groups as catalytic centers has also been considered (mechanism c in the Sup-

porting Information). Interestingly, when a carboxylic group acts as a catalytic center, scission of hydride to form H_2 by protonation with a TFA molecule is kinetically prohibitive.

Overall, although we cannot rule out other possible mechanisms that may explain the observed reactivity, all data are fully consistent with the proposal that oxidized carbon fibers assist hydride transfer in a manner that is very close to how nature performs the same feat in pathways mediated by NADH or NADPH.

Reactivity of carbon fibers as hydride donor versus benzaldehyde as organic hydride acceptor

As final evidence for the formation of a hydride donor species on the surface of carbon fibers at negative potentials, we investigated the reduction of benzaldehyde. This organic substrate typically evolves towards formation of benzylic alcohol by a reduction process initiated by a hydride transfer.[57]

As a first set of experiments, we performed the linear-sweep voltammetry measured for solutions containing different concentrations of TFA (20 mM and 2 mM) in acetonitrile in the presence or absence of an excess of benzaldehyde (160 mM). All experiments were carried out using oxidized carbon fiber brushes as working electrodes at potentials between 0.0 and −0.7 V vs. Ag/AgCl at a scan rate of 10 $mV\,s^{-1}$ (Figure 8). Interestingly, at a higher concentration of TFA (20 mM), intensity is independent of the presence of benzaldehyde in the reaction medium. However, at a lower concentration of TFA (2 mM), the presence of benzaldehyde results in an increase in the measured intensity, suggesting the involvement of benzaldehyde in the electron-transfer process. These observations indicate a competition between hydride transfer to the protons (from TFA) or to the organic substrate (benzaldehyde).

Considering that hydride transfer to proton from TFA (i.e., hydrogen evolution) is a competitive reaction versus hydrogenation of benzaldehyde, we considered water as an alternative proton source necessary to generate the corresponding hydride. Thus, we tested the oxidized brush electrode by chronoamperometry in acetonitrile at −0.5 V vs. Ag/AgCl in a system containing water (1 M) and benzaldehyde (16 mM) and $NaClO_4$ 0.2 M as inert electrolyte. After 12 h, the benzaldehyde has been completely reduced to benzyl alcohol (Scheme 2 and Figure S12). In contrast, under the same experimental conditions, after 24 hours, using pristine carbon fiber as electrode, no benzyl alcohol was detected (Figure S13). Therefore, these data are consistent with our mechanistic proposal in which a species able to transfer hydrides is generated at the correct electrochemical potential. In addition, our experiments confirm the notion that the oxidation of the carbon fiber brushes is necessary to generate such active intermediate able to transfer hydrides to either protons (hydrogen evolution) or organic substrates (hydrogenation). Furthermore, the balance between these two possible processes can be modulated by controlling the acidity of the proton source. Thus, the more acidic additive (TFA) promotes hydrogen evolution, whereas the less acidic molecule (water) makes possible hydrogenation of organic substrates.

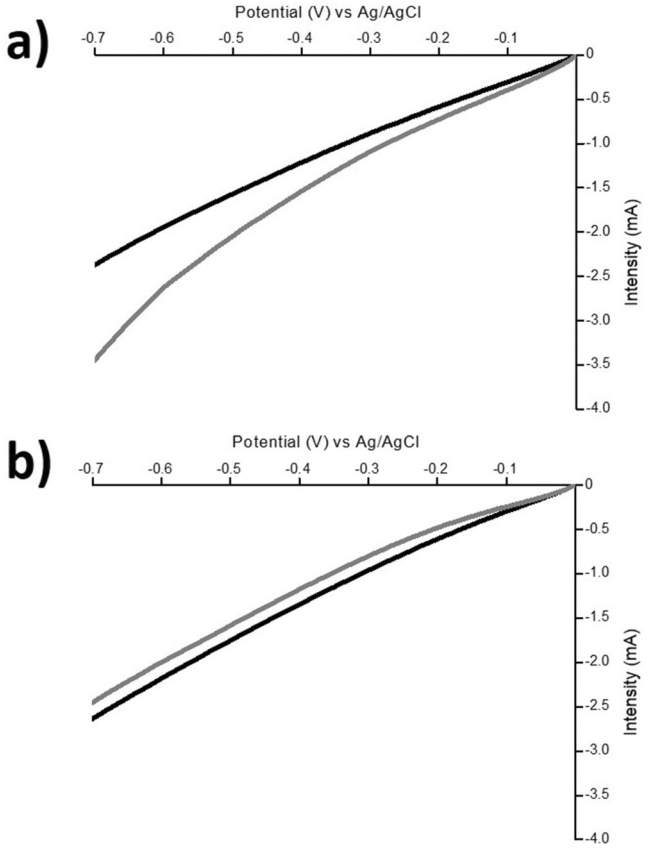

Figure 8. Linear voltammetry measured using oxidized carbon fiber electrodes in the absence (black) and in the presence (gray) of 160 mM benzaldehyde in CH_3CN (0.1 M $N(Bu)_4PF_6$) with TFA a) 2 mM or b) 20 mM.

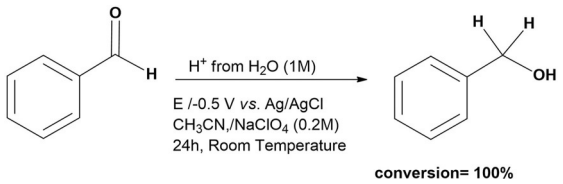

Scheme 2. Electrolytic reduction of benzaldehyde using oxidized carbon fiber brush electrode as working electrode in CH_3CN (0.2 M $NaClO_4$) with the presence of H_2O (1 M) and benzaldehyde 16 mM.

Conclusions

The combination of good electrical conductivity and the existence of chemical reactive sites, as a result of the presence of pyridinic nitrogen atoms on the surface of commercial carbon fibers, allows the design of new chemically modified electrodes with predetermined properties. Indeed, the oxidative functionalization of carbon fiber electrodes results in the formation of carboxylic groups, which are responsible for the efficient electrocatalytic generation of H_2 with quantitative faradaic yields and high current densities. The combination of experiments and calculations suggests that oxidized carbon fibers act as electrocatalysts in a bioinspired manner. The collected data led to the proposal that some of the carboxylic groups generated from oxidation process can be located *meta* to the pyridinic nitrogen atom, generating a nicotinic fragment. Such fragment

assists the formation and scission of hydride, which can easily evolve to molecular hydrogen through protonation. Moreover, hydride transfer mediated by oxidized carbon fibers can also be performed towards the reduction of organic substrates such as benzaldehyde.

Overall, we have reported a very inexpensive carbon-based alternative material that can be used as a modified electrode through easy manipulations that avoid coverage and/or deposition of materials into the electrodes, allowing the design of a reduced device with a high effective area able to produce H_2 in large amounts.

Experimental Section

Materials

All reagents, solvents, and materials were purchased from commercial sources and used without further purification. Specifically, fabric of carbon fiber (Twill 2×2 3 K weight 200 gr m^{-2} width 1200 mm, Model HA2301) was purchased from ClipCarbono.

Electrode preparation

The commercial carbon fiber was turned seven times around a 3 cm plastic strip to make a 6 cm long bunch of fibers. It was then joined to a copper wire and finally everything was made tight with Teflon tape. The electrodes were hand-made, but we tried to make them as homogeneously as possible to maintain the same design. The ready-made electrodes were held for 30 min in commercial sulfuric acid (98%) at RT with stirring and then placed into a mixture 1:1 of H_2SO_4/H_2O_2. The H_2O_2 was fresh and the mixture with H_2SO_4 was prepared a few minutes before use. If the mixture was not ready-made the oxidative potential of the reactive mixture was not sufficient to oxidize the carbon fiber. The electrodes were washed and sonicated in distilled water to remove all acid traces among fibers; this required several washing cycles. When the pH of the water was constant, the electrodes were sonicated for 10–15 min in either isopropanol or ethanol and dried with a heat gun.

Photoelectron spectroscopy (XPS)

Spectra were obtained with a VG Escalab 200R spectrometer equipped with a hemispherical electron analyzer (pass energy of 50 eV) and an Mg Kα ($h\nu$ = 1254.6 eV, 1 eV = 1.6302×10^{-19} J) X-ray source, powered at 120 W. The kinetic energies of photoelectrons were measured using a hemispherical electron analyzer working in the constant pass energy mode. The background pressure in the analysis chamber was kept below 6×10^{-9} mbar during data acquisition. The XPS data signals were taken in increments of 0.1 eV with dwell times of 50 ms. Binding energies were calibrated relative to the C 1s peak at 284.8 eV. High-resolution spectra envelopes were obtained by curve fitting synthetic peak components using the software XPS peak. The raw data were used with no preliminary smoothing. Symmetric Gaussian–Lorentzian product functions were used to approximate the line shapes of the fitting components. Morphological characterizations of the carbon fiber were carried out using a scanning electron microscope (Philips XL30 S-FEG). Measurements of the fiber diameter were done using ImageJ software. Identification of the chemical elements that were contained in the carbon fiber was conducted in a total reflection X-ray fluorescence (TXRF) 8030c-FEI spectrometer. A Mo Kα X-ray source was used as energy source at 50 kV and 0.6 mA.

Electrochemistry

Electrochemical experiments were performed under an argon atmosphere at RT in CH_3CN or water solutions. Tetrabutylammonium hexafluorophosphate (Bu_4NPF_6) or sodium perchlorate ($NaClO_4$) were used as supporting electrolytes. Measurements were carried out with an Ivium CompaqStat potentiostat interfaced with a computer. A standard three-electrode electrochemical cell was used. Potentials are referred to an Ag/AgCl, Et_4NBr 0.4 M reference electrode in ethylene glycol, and measured potentials were calibrated using an internal Fc/Fc+ standard. The working electrode was a carbon fiber brush. The auxiliary electrode was a pristine carbon fiber brush.

Gas chromatography

The evolved amount of H_2 during the electrocatalytic reaction was monitored approximately every 4 min by gas chromatography, by injecting samples of the internal atmosphere into an Agilent 490 micro gas chromatograph equipped with a thermal conductivity detector and a 1/8" Molesieve 100/120 column, calibrated with different H_2/He/CO/CH_4 mixtures of known composition. For gas chromatography quantification of alcohol benzaldehyde, 0.1 mL of the solution was mixed with 0.2 mL of methyl-naphthalene as standard and 0.7 mL chloroform. A calibration of benzyl alcohol was carried out in the range of 1×10^{-6} to 1×10^{-5} moles using the same amount of standard, enabling the quantification of the benzyl alcohol amount. Analysis was performed with an Agilent 7820A GC system equipped with a mass spectroscopy detector (5977B MSD).

Nuclear magnetic resonance

The amount of benzylic alcohol generated was quantified during the chronoamperommetry experiment by extracting samples of 1 mL of reaction mixture. CH_3CN solvent was removed under vacuum. Chloroform (1 mL) was added, which dissolved the organic compounds but not the inorganic salt. Finally, the solution was filtered (0.45 μm pore size) and analyzed by ^{1}H NMR spectroscopy and gas chromatography. Spectra were acquired with a Bruker 300 spectrometer running at 300 MHz for ^{1}H. Chemical shifts (δ) are reported in ppm relative to residual solvent signal ($CDCl_3$: δ = 7.26 ppm).

Scanning electron microscopy (SEM)

Morphological characterizations of the carbon fiber were carried out using a scanning electron microscope (Philips XL30 S-FEG). Measurements of the fiber diameter were done using ImageJ software.

Total reflection X-ray fluorescence (TXRF)

Identification of the chemical elements that were contained in the carbon fiber was conducted with a TXRF 8030c-FEI Spectrometer. A Mo Kα X-ray source was used as energy source at 50 kV and 0.6 mA.

Acknowledgements

This work was supported by the Spanish Ministerio de Economia *y* Competitividad (MINECO) (CTQ2016-76061-P and CTQ2015-64561-R), the European Research Council (StG 239910 and CG-2014-648304), and the Generalitat de Catalu-

nya (2014 SGR 862 and ICREA Academia award to M.C.). J.L.-F. thanks the CELLEX foundation for the starting career program for financial support. Financial support from the MINECO through the "Maria de Maeztu" Program for Units of Excellence in R&D (MDM-2014-0377) is also acknowledged. We are very grateful to Dr. Sergio Diaz-Tendero for many fruitful discussions. We acknowledge the generous allocation of computer time at the Centro de Computación Científica at the Universidad Autónoma de Madrid (CCC-UAM).

Conflict of interest

The authors declare no conflict of interest.

Keywords: biomimetic chemistry · electrochemistry · hydrides · hydrogen · materials science

[1] B. Alberts, D. Bray, J. Lewis, M. Raff, K. Roberts, J. D. Watson, in *Molecular Biology of the Cell*, 3rd ed., Garland, New York, **2002**.
[2] J. M. Berg, J. L. Tymoczko, L. Stryer, *Biochemistry*, W. H. Freeman, New York, 5th ed., **2002**.
[3] H. Adolfsson, *Angew. Chem. Int. Ed.* **2005**, *44*, 3340 – 3342; *Angew. Chem.* **2005**, *117*, 3404 – 3406.
[4] J. Rosen, *Chemtracts* **2005**, *18*, 65 – 71.
[5] S.-L. You, *Chem. Asian J.* **2007**, *2*, 820 – 827.
[6] S. G. Ouellet, A. M. Walji, D. W. C. Macmillan, *Acc. Chem. Res.* **2007**, *40*, 1327 – 1339.
[7] S. J. Connon, *Org. Biomol. Chem.* **2007**, *5*, 3407 – 3417.
[8] C. Wang, X. Wu, J. Xiao, *Chem. Asian J.* **2008**, *3*, 1750 – 1770.
[9] M. Rueping, E. Sugiono, F. R. Schoepke, *Synlett* **2010**, 852 – 865.
[10] M. Rueping, J. Dufour, F. R. Schoepke, *Green Chem.* **2011**, *13*, 1084 – 1105.
[11] D. G. Nocera, *Inorg. Chem.* **2009**, *48*, 10001 – 10017.
[12] M. G. Walter, E. L. Warren, J. R. McKone, S. W. Boettcher, Q. Mi, E. A. Santori, N. S. Lewis, *Chem. Rev.* **2010**, *110*, 6446 – 6473.
[13] M. Zeng, Y. Li, *J. Mater. Chem. A* **2015**, *3*, 14942 – 14962.
[14] Y. Zheng, Y. Jiao, M. Jaroniec, S. Z. Qiao, *Angew. Chem. Int. Ed.* **2015**, *54*, 52 – 65; *Angew. Chem.* **2015**, *127*, 52 – 66.
[15] W. Sheng, Z. Zhuang, M. Gao, J. Zheng, J. G. Chen, Y. Yan, *Nat. Commun.* **2015**, *6*, 5848.
[16] W. Sheng, H. A. Gasteiger, Y. Shao-Horn, *J. Electrochem. Soc.* **2010**, *157*, B1529 – B1536.
[17] X. Zou, Y. Zhang, *Chem. Soc. Rev.* **2015**, *44*, 5148 – 5180.
[18] Y. Hou, B. L. Abrams, P. C. K. Vesborg, M. E. Björketun, K. Herbst, L. Bech, A. M. Setti, C. D. Damsgaard, T. Pedersen, O. Hansen, J. Rossmeisl, S. Dahl, J. K. Nørskov, I. Chorkendorff, *Nat. Mater.* **2011**, *10*, 434 – 438.
[19] K. S. Novoselov, V. I. Falko, L. Colombo, P. R. Gellert, M. G. Schwab, K. Kim, *Nature* **2012**, *490*, 192 – 200.
[20] K. R. Paton, E. Varrla, C. Backes, R. J. Smith, U. Khan, A. O'Neill, C. Boland, M. Lotya, O. M. Istrate, P. King, T. Higgins, S. Barwich, P. May, P. Puczkarski, I. Ahmed, M. Moebius, H. Pettersson, E. Long, J. Coelho, S. E. O'Brien, E. K. McGuire, B. M. Sanchez, G. S. Duesberg, N. McEvoy, T. J. Pennycook, C. Downing, A. Crossley, V. Nicolosi, J. N. Coleman, *Nat. Mater.* **2014**, *13*, 624 – 630.
[21] M.-R. Azani, A. Hassanpour, V. Carcelén, C. Gibaja, D. Granados, R. Mas-Ballesté, F. Zamora, *Appl. Mater. Today* **2016**, *2*, 17 – 23.
[22] S. Navalón, J. R. Herance, M. Álvaro, H. García, *Chem. Eur. J.* **2017**, *23*, 15244 – 15275.
[23] Y. Xu, M. Kraft, R. Xu, *Chem. Soc. Rev.* **2016**, *45*, 3039 – 3052.
[24] W. Zhou, J. Jia, J. Lu, L. Yang, D. Hou, G. Li, S. Chen, *Nano Energy* **2016**, *28*, 29 – 43.
[25] J. Hu, C. Zhang, X. Meng, H. Lin, C. Hu, X. Long, S. Yang, *J. Mater. Chem. A* **2017**, *5*, 5995 – 6012.
[26] V. R. Stamenkovic, D. Strmcnik, P. P. Lopes, N. M. Markovic, *Nat. Mater.* **2017**, *16*, 57 – 69.
[27] W. Cui, Q. Liu, N. Cheng, A. M. Asiri, X. Sun, *Chem. Commun.* **2014**, *50*, 9340 – 9342.
[28] Q. Liu, J. Tian, W. Cui, P. Jiang, N. Cheng, A. M. Asiri, X. Sun, *Angew. Chem. Int. Ed.* **2014**, *53*, 6710 – 6714; *Angew. Chem.* **2014**, *126*, 6828 – 6832.
[29] R. K. Das, Y. Wang, S. V. Vasilyeva, E. Donoghue, I. Pucher, G. Kamenov, H.-P. Cheng, A. G. Rinzler, *ACS Nano* **2014**, *8*, 8447 – 8456.
[30] J. K. Kim, G. D. Park, J. H. Kim, S.-K. Park, Y. C. Kang, *Small* **2017**, *13*, 1700068.
[31] A. Xie, N. Xuan, K. Ba, Z. Sun, *ACS Appl. Mater. Interfaces* **2017**, *9*, 4643 – 4648.
[32] G. Valenti, A. Boni, M. Melchionna, M. Cargnello, L. Nasi, G. Bertoni, R. J. Gorte, M. Marcaccio, S. Rapino, M. Bonchio, P. Fornasiero, M. Prato, F. Paolucci, *Nat. Commun.* **2016**, *7*, 13549.
[33] J. D. Blakemore, A. Gupta, J. J. Warren, B. S. Brunschwig, H. B. Gray, *J. Am. Chem. Soc.* **2013**, *135*, 18288 – 18291.
[34] Commercial carbon fiber, http://www.clipcarbono.com/es/home/266-tejido-de-fibra-de-carbono-sarga-2×2-3k-peso-200gr-m2-ancho-1200-mm.html.
[35] M. S. A. Rahaman, A. F. Ismail, A. Mustafa, *Polym. Degrad. Stab.* **2007**, *92*, 1421 – 1432.
[36] L.-G. Tang, J. L. Kardos, *Polym. Compos.* **1997**, *18*, 100 – 113.
[37] E. Pamula, P. G. Rouxhet, *Carbon* **2003**, *41*, 1905 – 1915.
[38] D. D. Edie, *Carbon* **1998**, *36*, 345 – 362.
[39] X. Huang, *Materials* **2009**, *2*, 2369 – 2403.
[40] R. Sengupta, M. Bhattacharya, S. Bandyopadhyay, A. K. Bhowmick, *Progr. Polymer Sci.* **2011**, *36*, 638 – 670.
[41] Y. Liu, S. Kumar, *Polym. Rev.* **2012**, *52*, 234 – 258.
[42] X. Zhang, L. Liu, M. Li, Y. Chang, L. Shang, J. Dong, L. Xiao, Y. Ao, *RSC Adv.* **2016**, *6*, 29428 – 29436.
[43] B. Gao, W. Du, R. Zhang, F. Lu, J. Zhang, *Mater. Lett.* **2016**, *179*, 16 – 19.
[44] G. Zhang, S. Sun, D. Yang, J.-P. Dodelet, E. Sacher, *Carbon* **2008**, *46*, 196 – 205.
[45] W. S. Hummers, R. E. Offeman, *J. Am. Chem. Soc.* **1958**, *80*, 1339 – 1339.
[46] A. B. Charette, *Handbook of Reagents for Organic Synthesis: Reagents for Heteroarene Functionalization*, Wiley, Hoboken, **2005**.
[47] J. R. Hanson, *Functional Group Chemistry* (Ed.: E. W. Abel), RSC, Cambridge, **2001**.
[48] F. A. Carey, R. J. Sundberg, *Advanced Organic Chemistry*, 5th ed., Springer, Berlin, **2008**.
[49] Gaussian 09, Revision E.01, M. J. Frisch, G. W. Trucks, H. B. Schlegel, G. E. Scuseria, M. A. Robb, J. R. Cheeseman, G. Scalmani, V. Barone, B. Mennucci, G. A. Petersson, H. Nakatsuji, M. Caricato, X. Li, H. P. Hratchian, A. F. Izmaylov, J. Bloino, G. Zheng, J. L. Sonnenberg, M. Hada, M. Ehara, K. Toyota, R. Fukuda, J. Hasegawa, M. Ishida, T. Nakajima, Y. Honda, O. Kitao, H. Nakai, T. Vreven, J. A. Montgomery, Jr., J. E. Peralta, F. Ogliaro, M. Bearpark, J. J. Heyd, E. Brothers, K. N. Kudin, V. N. Staroverov, R. Kobayashi, J. Normand, K. Raghavachari, A. Rendell, J. C. Burant, S. S. Iyengar, J. Tomasi, M. Cossi, N. Rega, J. M. Millam, M. Klene, J. E. Knox, J. B. Cross, V. Bakken, C. Adamo, J. Jaramillo, R. Gomperts, R. E. Stratmann, O. Yazyev, A. J. Austin, R. Cammi, C. Pomelli, J. W. Ochterski, R. L. Martin, K. Morokuma, V. G. Zakrzewski, G. A. Voth, P. Salvador, J. J. Dannenberg, S. Dapprich, A. D. Daniels, Ö. Farkas, J. B. Foresman, J. V. Ortiz, J. Cioslowski, D. J. Fox, Gaussian, Inc., Wallingford CT, **2016**.
[50] T. Ziegler, *Chem. Rev.* **1991**, *91*, 651 – 667.
[51] Y. Zhao, D. G. Truhlar, *Theor. Chem. Acc.* **2008**, *120*, 215 – 241.
[52] Y. Zhao, D. G. Truhlar, *Acc. Chem. Res.* **2008**, *41*, 157 – 167.
[53] W. R. Fawcett, *Langmuir* **2008**, *24*, 9868 – 9875.
[54] A. V. Marenich, C. J. Cramer, D. G. Truhlar, *J. Phys. Chem. B* **2009**, *113*, 6378 – 6396.
[55] M. Shiraishi, M. Ata, *Carbon* **2001**, *39*, 1913 – 1917.
[56] L. Simón, J. M. Goodman, *J. Am. Chem. Soc.* **2008**, *130*, 8741 – 8747.
[57] A. Proto, R. Cucciniello, A. Genga, C. Capacchione, *Catal. Commun.* **2015**, *68*, 41 – 45.

Manuscript received: November 28, 2017
Accepted manuscript online: January 3, 2018
Version of record online: February 5, 2018